Inhibition of c-*src* Transcription by Mithramycin: Structure−Activity Relationships of Biosynthetically Produced Mithramycin Analogues Using the c-*src* Promoter as Target†

Lily L. Remsing,‡ Hamid R. Bahadori,§ Giuseppina M. Carbone,§ Eileen M. McGuffie,§ Carlo V. Catapano,§ and Jürgen Rohr*,‡

Division of Pharmaceutical Sciences, College of Pharmacy, University of Kentucky, Lexington, Kentucky 40536, and Laboratory of Cancer Genomics, Hollings Cancer Center and Department of Medicine, Hematology/Oncology Division, Medical University of South Carolina, Charleston, South Carolina 29425

Received January 16, 2003; Revised Manuscript Received May 20, 2003

ABSTRACT: The aureolic acid antitumor antibiotic mithramycin (MTM) inhibits both cancer growth and bone resorption by cross-linking GC-rich DNA, thus blocking binding of Sp-family transcription factors to gene regulatory elements. Transcription of c-*src*, a gene implicated in many human cancers and required for osteoclast-dependent bone resorption, is regulated by the binding of Sp factors to specific elements in its promoter. Therefore, this gene represents an important anticancer target *and* a potential lead target through which MTM displays its so far uncharacterized action against osteoclastic bone resorption. Here we demonstrate, using DNA binding studies, promoter reporter assays, and RT-PCR, that MTM inhibits Sp binding to the c-*src* promoter region, thereby decreasing its expression in human cancer cells. Furthermore, selected mithramycin analogues, namely, premithramycin B, mithramycin SK, 7-demethylmithramycin, 4E-ketomithramycin, and 4C-ketodemycarosylmithramycin, generated through combinatorial biosynthesis, were compared with MTM for their ability to block Sp binding to the c-*src* promoter. Although most of the tested compounds lost their ability to bind to the DNA, alteration of the MTM 3-pentyl side chain led to a compound (mithramycin SK) with the same DNA binding specificity but with lower binding affinity than MTM. While this compound was comparable to MTM in promoter reporter, gene expression, and anticancer assays, given its weaker interaction with the DNA, it may be much less toxic than MTM. The results presented here supplement recent findings and, moreover, allow new conclusions to be made regarding both the structure−activity relationships, particularly with respect to the alkyl side chains, and the mechanism of action of aureolic acid drugs.

Mithramycin (**1**, MTM,[1] also known as aureolic acid, mithracin, LA-7017, PA-144, and plicamycin; see Figure 1) is an aureolic acid-type polyketide produced by the soil bacteria *Streptomyces argillaceus* (ATCC 12956). The aureolic acid group of anticancer antibiotics includes MTM, chromomycin A_3 (**2**, CHR), olivomycin A (**3**, OLI), UCH9 (**4**), and the newly discovered durhamycin A (**5**, DUR) (*1*). All contain the same tricyclic core moiety with a unique dihydroxymethoxyoxopentyl side chain attached at C-3 and vary only slightly with respect to the residue at C-7, which is either a H-atom or a small alkyl side chain. However, they differ in the nature and linking of their saccharide chains, which consist of various 2,6-dideoxy sugar residues (*2*). These structural variations impart subtle differences in the DNA binding and activity profiles among the members of this group (*3*−*7*). CHR has been used in Japan (in combination with other antitumor drugs) for the treatment of solid tumors, particularly advanced stomach cancers. In Russia, testicular and tonsilar malignancies have been treated with OLI (*4*). MTM has been used clinically in the United States to treat Paget's disease and testicular carcinoma (*8*−*11*). In addition, its hypocalcemic effect has been used to manage hypercalcemia in patients with malignancy-associated bone lesions (*12*). The anticancer activity of MTM has been associated with its ability to inhibit replication and transcription via cross-linking of the DNA strands, thereby blocking its template activity for DNA- and RNA-dependent polymerases (*8*, *13*). Recent studies have suggested a more specific mechanism for MTM activity based on its ability to bind preferentially to GC-rich DNA. In this manner, MTM

† This work was supported by National Institutes of Health Grant 1RO1CA091901-01 (to J.R.) and a grant from the Department of Defense, Coastal Carolina Thoracic Cancer Program (to C.V.C.).

* To whom correspondence should be addressed. Phone: (859) 323-5031. Fax: (859) 257-7564. E-mail: jrohr2@uky.edu.

‡ University of Kentucky.

§ Medical University of South Carolina.

[1] Abbreviations: bp, base pair(s); 4C-K, 4C-ketodemycarosylmithramycin; 4E-K, 4E-ketomithramycin; 7-DM, 7-demethylmithramycin; DMSO, dimethyl sulfoxide; DOTAP, [*N*-[1-(2,3-dioleoyloxy)]-*N*,*N*,*N*-trimethylammonium]propane methyl sulfate; DTT, dithiothreitol; DUR, durhamycin; EDTA, ethylenediaminetetraacetic acid; EMSA, electrophoretic mobility shift assay; GAPDH, glyceraldehyde-3-phosphate dehydrogenase; GI_{50}, growth inhibitory effect; HEPES, 4-(2-hydroxyethyl)-1-piperazineethanesulfonic acid; MTM, mithramycin; MTT, 3-(4,5-dimethylthiazol-2-yl)-2,5-diphenyltetrazolium bromide; RT-PCR, reverse transcriptase−polymerase chain reaction; PKS, polyketide synthase; Pre-B, premithramycin B; PTK, protein tyrosine kinase; SAR, structure−activity relationships; SK, mithramycin SK; TBE, Tris−borate/EDTA electrophoresis buffer; TBM, Tris−borate/magnesium chloride buffer.

10.1021/bi034091z CCC: $25.00
Published on Web 06/20/2003

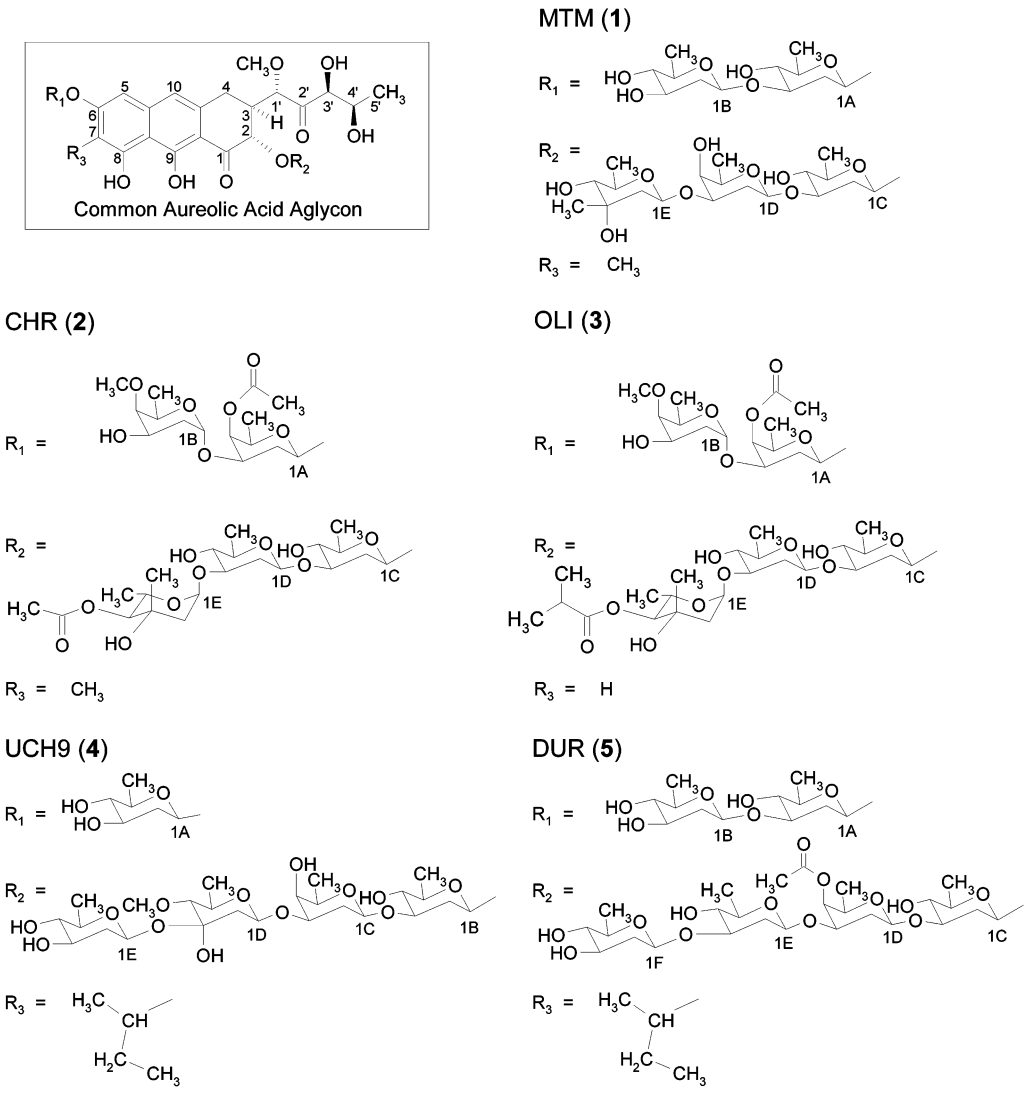

FIGURE 1: Structures of natural aureolic acid compounds: MTM (**1**) = mithramycin, CHR (**2**) = chromomycin A_3, OLI (**3**) = olivomycin, UCH9 (**4**), and DUR (**5**) = durhamycin.

has been shown to interfere with DNA binding proteins, such as Sp-family transcription factors, which specifically interact with GC-rich DNA sequences, and inhibit expression of Sp1-regulated genes such as, among others, the c-*myc* proto-oncogene, the SV40 early promoter, the dihydrofolate reductase gene, and the collagen-α1(I) gene (*8*, *14*−*21*). In the latter instance, MTM was found to selectively inhibit Sp1 binding, while binding of the NF-I transcription factor, which recognizes the CCAAT box, was unaffected (*18*). Another proto-oncogene that requires Sp1 binding for mRNA synthesis is the c-*src* proto-oncogene (*22*), the overexpression of which has been implicated in malignancies of the colon, breast, pancreas, lung, and brain (*23*, *24*). In addition, expression of c-*src* is required for the bone-resorbing function of osteoclasts as illustrated by the development of osteopetrosis in c-*src* knockout mice (*25*). Interestingly, MTM has been shown to inhibit bone resorption by preventing the synthesis of a hitherto unidentified mRNA in the osteoclast (*26*). Given c-*src*'s dependence on Sp1 binding, as well as its involvement in osteoclast function, we propose that this gene represents not only another important MTM anticancer target but also a potential lead target through which MTM displays its action against osteoclast-dependent bone resorption. Thus, the first objective of this study was to show that MTM inhibits the transcription of the c-*src* proto-oncogene by blocking the binding of Sp transcription factors to its promoter region.

Taking into account the fact that all aureolic acid drugs exhibit severe side effects, including gastrointestinal, hepatic, renal, and bone marrow toxicities (*9*, *27*), the second objective of this study was to search for MTM analogues with lower toxicity levels, higher biological activity, or both. Although synthetic and semisynthetic approaches toward the production of new aureolic acid-type compounds are feasible, a more versatile method is a combinatorial biosynthetic procedure whereby the genes of the biosynthetic pathway of the drugs are altered in the bacteria themselves (e.g., through gene inactivation, recombination, or multiplication). Applying the methods of combinatorial biosynthesis on the MTM producer *S. argillaceus* (ATCC 12956) yielded various MTM derivatives exhibiting an array of structural changes in the saccharide chains as well as in the aglycon moiety (tetracyclic vs tricyclic and/or modifications in the alkyl side chains) (*28*−*32*), which presumably correspond to altered biological activities. These newly biosynthesized MTM analogues not only are a good source for information

regarding the structure−activity relationships (SAR) of MTM but may even reveal a compound possessing a superior therapeutic index compared to MTM, as well as the bacterial strain for the compound's biotechnological production.

Therefore, MTM and selected MTM analogues, generated through combinatorial biosynthetic methods in previous studies, were investigated for their effect on Sp binding to the c-*src* promoter region. We used DNase I "footprinting", one of several techniques generally used to determine sites of protein binding to DNA but which has also been employed to map the preferred binding sites of DNA binding drugs such as MTM (*5*, *33*−*37*), to determine the ability of the selected compounds to bind to the c-*src* promoter region. Electrophoretic mobility shift assays (EMSA) were used to monitor the ability of the selected compounds to block the binding of Sp transcription factors. Subsequent downregulation of c-*src* promoter activity and gene expression was monitored by promoter reporter analysis and RT-PCR, respectively. In addition, cytotoxicity assays were performed with various human tumor cell lines to gain insights into the anticancer activity of the new MTM analogues. In the process, we were able to garner valuable information regarding the SAR of mithramycin-type compounds that will aid in the future development of clinically useful MTM derivatives.

EXPERIMENTAL PROCEDURES

Compounds Tested. Mithramycin (**1**), premithramycin B (**6**) (*32*), mithramycin SK (**7**) (*31*), 7-demethylmithramycin (**8**) (*29*), 4E-ketomithramycin (**9**) (*30*), and 4C-ketodemycarosylmithramycin (**10**) (*28*, *30*) were available from previous experiments. The six compounds were prepared in sterile DMSO as 10 mM stock solutions and stored at −20 °C. Desired concentrations for each experiment were achieved by diluting the stock solution with sterile deionized water.

DNase I Footprinting. Experiments were performed on a 223 bp DNA fragment containing a portion of the c-*src* promoter region, which encompassed the known Sp binding sites (*22*). A *Kpn*I−*Xba*I fragment containing the functional promoter region of the human c-*src* gene was excised from p0.54Src-CAT (*38*) and subcloned into the pGEM-3Z vector (Promega, Madison, WI) to form pGEM-SRC. An inner portion of the c-*src* promoter region was then amplified from pGEM-SRC using the following primers: 5′-CTGGGGGCGGATGGGGCCCGCGGG**CTGCAG**CGCCCTG-3′ for the 5′ end of the region and 5′-GAGGAGGAGGAGGA**GGATCC**GGCGGCGGCCC-3′ for the 3′ end of the region. *Pst*I and *Bam*HI sites (noted in bold), respectively, were incorporated to facilitate subcloning of the PCR product into the same sites of pUC19 (New England Biolabs, Beverly, MA) to form the pUC19-PBSRC vector. Subsequent digestion of this vector with *Pst*I and *Bam*HI resulted in a 223 bp fragment, which was purified by agarose gel electrophoresis using the Qiaquick gel extraction kit (Qiagen, Valencia, CA). The *Bam*HI 5′-overhang was filled in using Klenow fragment (Promega) and [α-^{32}P]dCTP (3000 Ci/mmol; Amersham Pharmacia Biotech, Piscataway, NJ), resulting in the DNA being labeled 3′ of the Sp binding sites (Figure 3). For footprinting, the end-labeled 223 bp fragment of c-*src* DNA (1 nM) was preincubated in 90 nM Tris−borate, pH 8, and 10 mM $MgCl_2$ (TBM buffer), with 0, 20, 50, or 100 μM compound or with 1% DMSO as control for 1 h on ice. Digestion was performed on ice for 1 min with 16.7 units/mL (final concentration) DNase I. Reactions were stopped by adding 1.5× reaction volume of denaturing formamide buffer and heating at 85 °C for 5 min followed by electrophoretic analysis on 10% polyacrylamide−7 M urea gels at 60 W for 1.5 h (Figure 4). Radiolabeled ϕX174 DNA/*Hin*fI dephosphorylated markers (Promega) were used for approximate size determination (Figure 4). In addition, an aliquot of the 223 bp fragment was sequenced using a ^{32}P-end-labeled primer (5′-CGGCGGCGGCCCGGGGAGGGGAAGAG-3′) complementary to the 3′ end of the fragment and the SequiTherm Excel II DNA sequencing kit (Epicenter Technologies, Madison, WI) following the supplier's instructions.

PCR Amplification. PCR reaction conditions were as follows: 300 ng of pGEM-SRC was mixed with 250 nM (final concentration) primer and 2.5 units of PfuTurbo DNA polymerase (Stratagene) in a total reaction volume of 50 μL containing 0.4 mM each dNTP, 2.5% DMSO, 20% glycerol, and 1× PfuTurbo buffer. A TECHNE Techgene (Denville Scientific, Metuchen, NJ) thermocycler was used to perform the polymerization reaction, which included an initial denaturation step of 1 min at 98 °C, followed by 30 cycles of 1 min at 98 °C, 1 min at 65 °C, and 2 min at 76 °C. After the 30 cycles, an additional extension step of 10 min at 76 °C was added.

Electrophoretic Mobility Shift Assays. Nuclear extracts were prepared from MCF-7 human breast cancer cells as previously described (*39*). Protein concentrations were determined to be 2−4 μg/μL by the Bradford method (Bio-Rad, Hercules, CA). PAGE-purified oligonucleotides corresponding to the GC1 and GA2 sites in the c-*src* promoter were purchased from Sigma Genosys (The Woodlands, TX). The sequence of the top strand of the GC1probe was 5′-TGGCGGAGTGG**GAGGCGGGGC**TTCTGTGCCCGGTGTCCCCAC-3′) (Sp binding site in bold). The sequence of the top strand of the GA2 probe was 5′-GGCTGCCTGCCGG**GCCCCTCCTC**CCAGCTCGCGCGCTCCCTCCCT-3′ (Sp binding site in bold). For duplex formation, one strand was 5′ end-labeled with [γ-^{32}P]ATP and T4 polynucleotide kinase (Promega) and then incubated with an equal amount of the complementary oligonucleotide for 15 min at 98 °C and allowed to cool slowly to room temperature. In reactions containing MTM or the MTM analogues, the double-stranded DNA (1 nM final concentration) was preincubated with 0, 5, 20, or 100 μM compound in the presence of 50 mM HEPES buffer (pH 7.4) containing 10 mM $MgCl_2$ for 1 h on ice before the addition of protein extract. The MCF-7 cell nuclear protein extract was preincubated on ice in the presence of binding buffer [10 mM HEPES (pH 7.4), 4% glycerol, 50 mM NaCl, 1 mM $MgCl_2$, 0.5 mM EDTA, and 0.5 mM DTT] and 1 μg of poly(dI-dC) for 10 min and then combined with the DNA and incubated for an additional 20 min at 10 °C. Binding reactions were analyzed on 4% polyacrylamide gels under nondenaturing conditions. Electrophoresis (Figure 5) was carried out at 10 °C at 200 V for 2 h using 0.5× TBE as running buffer. For assignment of the Sp1− and Sp3−DNA band shifts, mobility shift reactions using Sp wild-type (competitive) and mutant (noncompetitive) double-stranded oligonucleotides, as well as Sp1 and Sp3 polyclonal antibodies, were performed using the Nushift

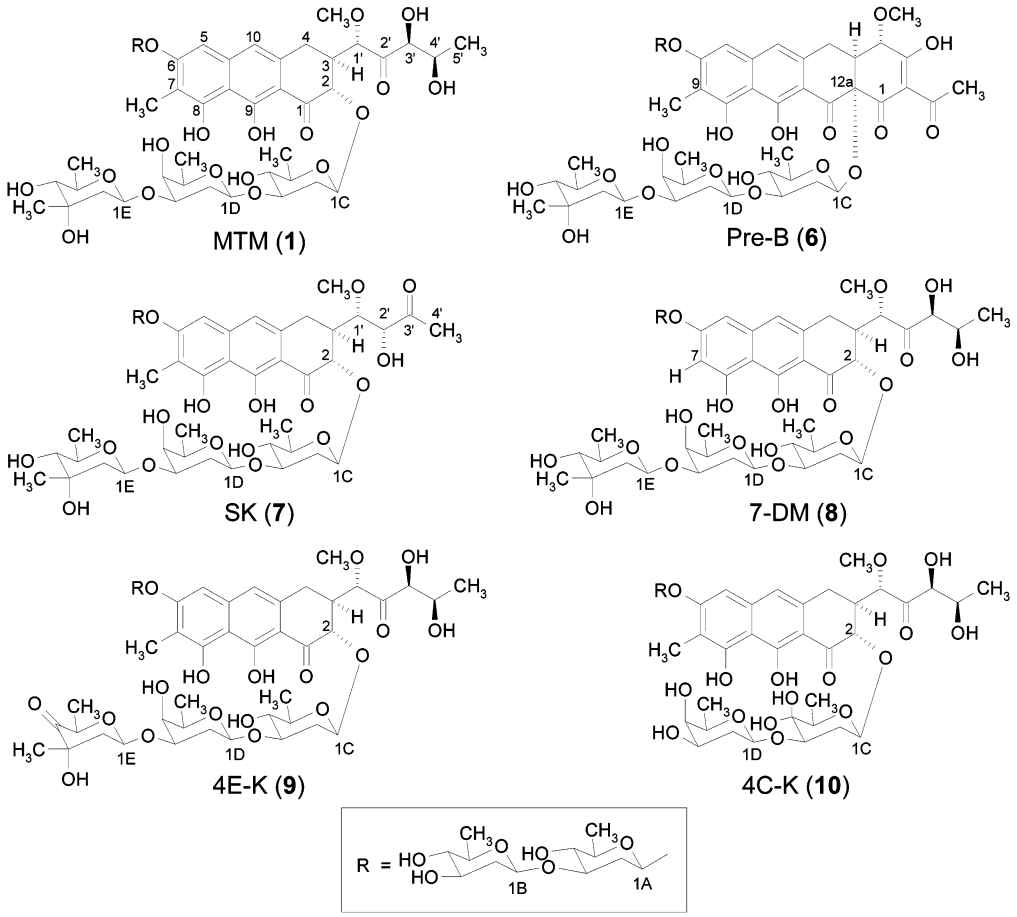

FIGURE 2: Stuctures of mithramycin analogues: MTM (**1**) = mithramycin, Pre-B (**6**) = premithramycin B, SK (**7**) = mithramycin SK, 7-DM (**8**) = 7-demethylmithramycin, 4E-K (**9**) = 4E-ketomithramycin, 4C-K (**10**) = 4C-ketodemycarosylmithramycin.

kit (Geneka Biotechnology, Montreal, Quebec, Canada). Normal rabbit IgG was used as a negative control. To address the issue of specificity, EMSAs were also performed using a consensus oligonucleotide for Oct1, an ubiquitous transcription factor that binds AT-rich DNA (*40*). The oligonucleotide, which included the Oct1 binding site (ATGCAAAT), was purchased from Promega and end-labeled according to Promega Technical Bulletin 110 using [γ-^{32}P]-ATP and T4 polynucleotide kinase. Preincubation with MTM or SK (0, 20, or 100 μM) and treatment with MCF-7 nuclear extract were performed as described above. For confirmation of the observed Oct1−DNA band shift, unlabeled Oct1 and Sp1 oligonucleotides were used for specific and nonspecific competition reactions, respectively.

Cell Culture. A549, H441, and H23 lung cancer cells, as well as the DU145 prostate cancer cells, were maintained in RPMI 1640 medium. MDA-MB-231 and MCF-7 breast cancer cells were grown in D-MEM medium. SW480 colon cancer cells were grown in McCoy's medium. All media were supplemented with 10% heat-inactivated fetal bovine serum (Invitrogen, Carlsbad, CA).

Transient Transfection and Luciferase Assay. For functional analysis of the c-*src* promoter region in the presence of MTM and its analogues, a *Kpn*I−*Hin*dIII fragment of 610 bp containing the functional promoter region of the human c-*src* gene was excised from p0.54Src-CAT (*38*) and subcloned into the luciferase reporter vector pGL3-Basic (Promega, Madison, WI) to form pGL3-SRC. A549 cells were plated at a density of 2×10^4 cells/well in 48-well plates. Cells were transfected with 200 ng of pGL3-SRC and 20 ng of pRL-CMV control vector (Promega) using the transfection reagent DOTAP (Roche, Indianapolis, IN) and a DOTAP:DNA ratio of 5:1. The pRL-CMV vector was added to monitor transfection efficiency. Plasmids and DOTAP were diluted in 20 mM Hepes, mixed, and incubated for 15 min at room temperature. The DOTAP/DNA mixture was then diluted with serum-containing medium and added to the cells. After 6 h of incubation, the medium was removed and replaced with fresh medium containing the indicated concentrations of each compound. Cells were incubated for an additional 24 h. Then, luciferase activity was measured in cell lysates using the Promega dual luciferase assay system following the manufacturer's instructions. Each treatment group was performed in triplicate.

RNA Extraction and RT-PCR. A549 were seeded in 6-well plates at a density of 1×10^5 cells/well and treated with MTM and MTM analogues 24 h later. Total RNA was extracted after 24 h of incubation using Trizol (Invitrogen). RNA concentrations were determined using a spectrophotometer. RT-PCR was performed with the SuperScript one-step RT-PCR system (Invitrogen) and 0.2 μM c-*src* and GAPDH specific primers. Sequences of forward and reverse primers for *c-src* were 5′-GTCTGACTTCGACAACGCCAAG-3′ and 5′-GAGAAAGTCCAGCAAA-3′. The amplified fragment was 493 bp long. RNA was reverse transcribed at 50 °C for 30 min and then subjected to 30 cycles of PCR (1. 15 s at 94 °C; 2. 30 s at 55 °C; and 3. 60 s at 72 °C). Primers and PCR conditions for GAPDH have been pub-

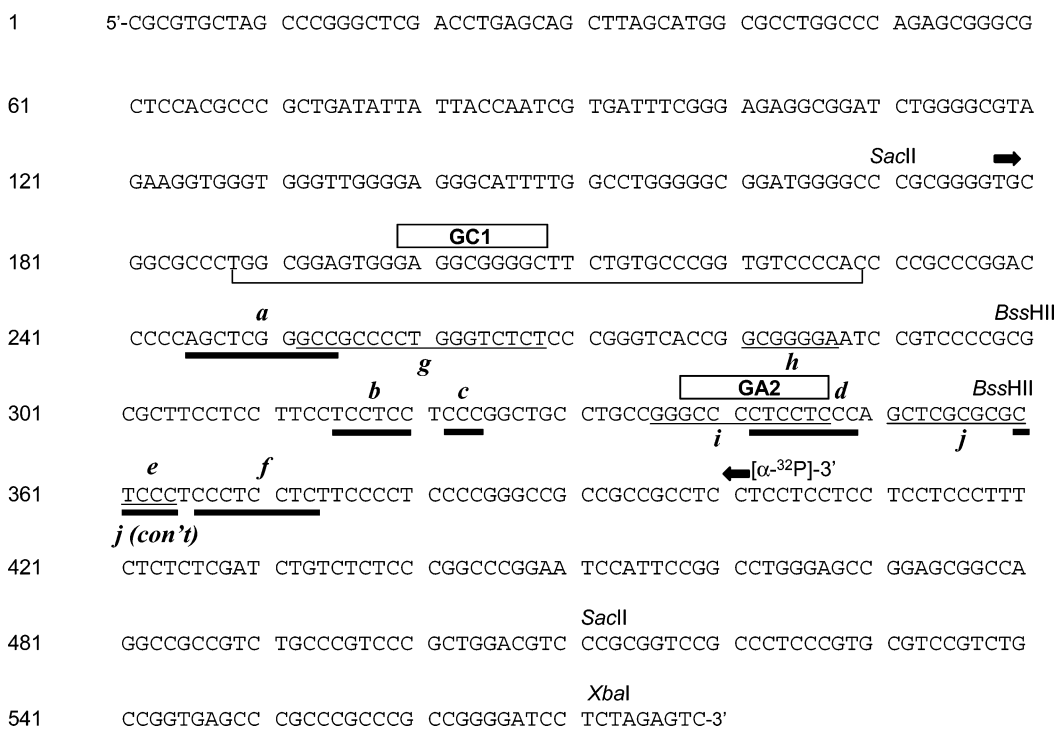

FIGURE 3: Sequence of the 579 bp c-*src* promoter region. Arrows indicate the 223 bp DNA fragment, which was labeled 3′ of the Sp1 binding sites. Lower case letters correspond to footprints in Figure 4. Thickly underlined sequences (a, b, c, d, e, and f) are footprints visible in the MTM and SK experiments. Thinly underlined sequences (g, h, i, and j) are footprints located in the 4C-K experiment. Boxes labeled GC1 and GA2 are reported Sp1 binding sites (*38*, *69*). The large bracket indicates regions included in the oligonucleotides used for EMSA. Assorted restriction sites are shown for reference.

lished previously (*41*). PCR products were analyzed on 2% agarose gels and visualized following ethidium bromide staining using a ChemiImager 4400 (AlphaInnotech, San Leandro, CA). Densitometric analysis was performed with AlphaEase software (AlphaInnotech).

Cell Proliferation Assay. Cells were seeded at a density of 1000−3000 cells/well in 96-well plates, grown for 24 h, and then incubated with the indicated analogue concentrations for 96 h. After 96 h, 25 μL of MTT (5 mg/mL in PBS) was added to each well, and the cells were incubated for 4 h as previously described (*41*). This was followed by overnight lysis at 37 °C. Absorbance was measured at 570 nm on a microplate reader. Each treatment group was performed in triplicate (see Figure 8).

RESULTS

Selection of MTM Analogues. The following MTM analogues were chosen for the investigations on the basis of their unique molecular alterations (Figure 2).

(A) Premithramycin B (**6**, Pre-B): Pre-B is the second latest intermediate of MTM biosynthesis. Only an oxidative cleavage of its C-1/C-2 bond followed by decarboxylation (loss of C-1) and a keto reduction step is necessary to finish the biosynthetic sequence to MTM. Although its tetracyclic structure is quite different from MTM, it shows an identical saccharide pattern and 7-side chain. However, Pre-B lacks the polyoxygenated pentyl side chain, since this is still "hidden" in the six-membered ring A and its 2-side chain. Thus, by comparing this compound with MTM, we expected to discern the impact of the conformationally flexible oxygenated pentyl side chain of MTM on its biological activity (*32*).

(B) Mithramycin SK (**7**, SK): SK is a new MTM analogue, whose structure elucidation and initial antitumor assay results are described in a separate publication (*31*). SK distinguishes itself from MTM by the shorter and functionally different 3-side chain. It has a butyl instead of a pentyl chain and the functional groups (keto and secondary alcohol) are in different positions (*31*). As with Pre-B, we expected to gain information about the importance of the 3-side chain in general. However, given that SK retains the flexible, albeit modified, side chain, the structural differences from MTM are less prominent than in Pre-B, thus permitting a more focused examination of this feature.

(C) 7-Demethylmithramycin (**8**, 7-DM): Structurally, this compound is almost identical with MTM; it lacks only the 7-methyl side chain (*29*). Thus, the latter's impact on MTM's biological activity can be directly evaluated through comparison of 7-DM with MTM.

(D) 4E-Ketomithramycin (**9**, 4E-K): 4E-K has a modified saccharide pattern. Specifically, the 4-OH group of sugar E has been replaced with a 4-keto function. Since sugar E seems to play an important role in the DNA interaction of MTM, a saccharide moiety modified in this unit seemed attractive. Given that 4E-K has a keto function in the 4E position versus the equatorially attached OH group found in MTM, this apex of the trisaccharide chain was converted from an H-bond donor into a H-bond acceptor (*30*).

(E) 4C-Ketodemycarosylmithramycin (**10**, 4C-K): 4C-K distinguishes itself in two ways from MTM. First, it lacks the last sugar (sugar E) of the saccharide chain attached at 2-O. Second, sugar C contains a (hydrated) keto function in the 4-position instead of an equatorial OH group (*30*). Thus, its structure will give further information about the impor-

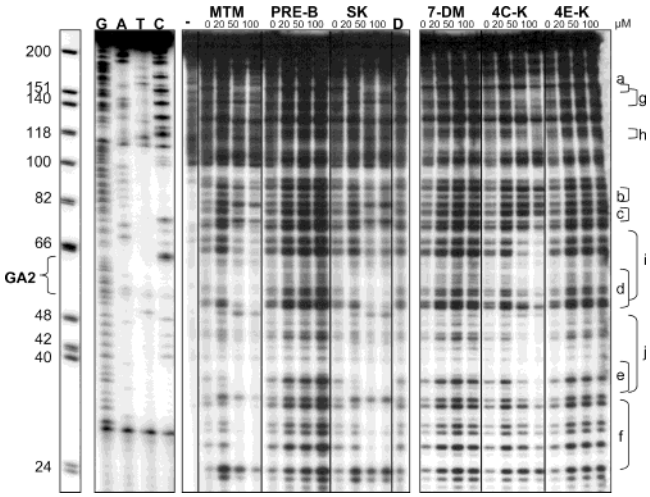

FIGURE 4: DNase I footprinting analysis of a 223 bp fragment of the c-*src* promoter in the presence of MTM and MTM analogues. End-labeled DNA was preincubated with the indicated amount of each compound or with 1% DMSO (D) as control for 1 h on ice. Digestion was performed on ice for 1 min with 16.7 units/mL (final concentration) DNase I and analyzed on 10% polyacrylamide−7 M urea gels. ^{32}P-Labeled ϕX174 DNA/*Hin*fI Marker (L) was used for approximate size determination. An aliquot of the 223 bp fragment was sequenced using a ^{32}P-end-labeled primer complementary to the 3′ (labeled) end of DNA used above. G = guanine; A = adenine; T = thymine; C = cytosine; − = no DNase. Lower case letters and brackets along the side of the gel represent footprints: a, b, c, d, e, and f are footprints visible in the MTM and SK experiments, while g, h, i, and j are located in the 4C-K experiment. MTM = mithramycin (**1**), Pre-B = premithramycin B (**6**), SK = mithramycin SK (**7**), 7-DM = 7-demethylmithramycin (**8**), 4E-K = 4E-ketomithramycin (**9**), and 4C-K = 4C-ketodemycarosylmithramycin (**10**).

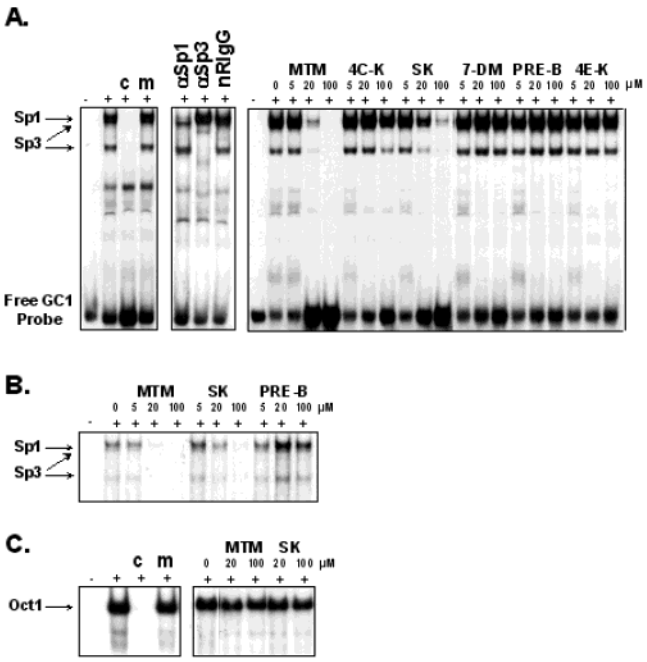

FIGURE 5: Effects of MTM and MTM analogues on Sp1/Sp3 binding to the c-*src* promoter. Panel A: In reactions containing MTM or the MTM analogues, the labeled duplex DNA corresponding to the GC1 Sp binding site of c-*src* was preincubated with the indicated amount of each compound in buffer (pH 7.4) containing 10 mM $MgCl_2$ for 1 h on ice before the addition of nuclear protein extract. The nuclear extract was preincubated on ice in the presence of binding buffer and poly(dI-dC) for 10 min and then combined with the DNA and incubated for an additional 20 min at 10 °C. Reactions were analyzed on 4% nondenaturing polyacrylamide gels. For assignment of the Sp1− and Sp3−DNA band shifts, mobility shift reactions using Sp wild-type (c) and mutant (m) double-stranded oligonucleotides, as well as Sp1 (αSp1) and Sp3 (αSp3) polyclonal antibodies, were performed. Normal rabbit IgG antibody (nRIgG) was used as a negative control. Panel B: To verify that both Sp binding sites were affected, MTM, SK, and PRE-B (0, 20, or 100 μM) were assayed as above using a probe for the GA2 Sp binding site. Panel C: To address the issue of specificity, a labeled consensus oligonucleotide for Oct1 was preincubated with MTM or SK (0, 20, or 100 μM) and treated with MCF-7 nuclear extract as described above. For confirmation of the observed Oct1−DNA band shift, unlabeled Oct1 (c) and Sp1 (m) oligonucleotides were used for specific and nonspecific competition reactions, respectively. − = no nuclear extract; + = with nuclear extract. MTM = mithramycin (**1**), Pre-B = premithramycin B (**6**), SK = mithramycin SK (**7**), 7-DM = 7-demethylmithramycin (**8**), 4E-K = 4E-ketomithramycin (**9**), and 4C-K = 4C-ketodemycarosylmithramycin (**10**).

tance of the trisaccharide side chain and its features in MTM and related drugs.

All of the MTM analogues were available through the constructed mutants described in the cited references [Pre-B (*32*), 7-DM (*29*), SK (*31*), 4C-K (*28*, *30*), and 4E-K (*30*)].

Selection of Target DNA. Figure 3 shows the sequence of the entire functional promoter region of the c-*src* proto-oncogene, including the two reported Sp binding sites, namely, GC1 and GA2 (*22*). These two sites, which are required for transcriptional activation of the c-*src* gene (*38*), are located approximately 205 and 345 bp, respectively, from the 5′ end of the DNA fragment. For comparison of the regions protected by the binding of MTM or the MTM analogues to the c-*src* DNA, DNase I treatment was performed on a 223 bp DNA segment of the c-*src* promoter region surrounding the two Sp binding sites (see Figure 3). The GC1 Sp binding site was used for the EMSAs, and the region corresponding to the oligonucleotide used in this assay is also indicated in Figure 3.

Binding Sites of MTM and Selected Compounds. To characterize the ability of MTM and the MTM analogues to bind to and protect the c-*src* DNA from DNase digest, we used the above-described 223 bp c-*src* DNA fragment. The resulting autoradiographs are shown in Figure 4. Six clear footprints or regions of DNase I protection (labeled a, b, c, d, e, and f) are visible in the experiments in which the c-*src* DNA was treated with MTM (**1**). The respective sequences of the MTM-produced footprints are identified in Figure 3. Upon investigation of the sequences, it is apparent that the characteristic selectivity of MTM for GC-rich DNA, particularly for the dinucleotide CC·GG, was maintained with this DNA target. Pre-B (**6**), 7-DM (**8**), and 4E-K (**9**) displayed similar results in that no footprints were formed. SK (**7**), on the other hand, produced footprints at the same sites and had efficacy comparable to that of MTM, particularly at the GA2 site. The results of the footprint experiments with 4C-K (**10**) made it clear that the loss of the mycarose moiety did not cause this compound to lose its ability to bind to the DNA target. It did appear to change the sequence recognition, however, resulting in several footprints (labeled g, h, i, and j), which were either unique from (h) or overlapping with (g, i, and j) footprints produced by MTM. In addition, several footprints produced by MTM (b, c, and f) were not produced by 4C-K. Of particular interest is the overlap of sites d (MTM) and i (4C-K), which correspond

to the GA2 Sp binding region as indicated in Figures 3 and 4. Although binding to the GC1 site was not observable in the DNase footprinting assay, results from the EMSA and the luciferase assay (described below) suggest that in the case of MTM and SK both Sp binding sites are protected.

Binding of Sp Transcription Factors to the c-src Promoter. To confirm the presence of c-*src* DNA−Sp protein complexes, EMSAs were performed using a labeled 42 bp DNA fragment (see Figure 3) including the GC1 Sp binding site from the c-*src* promoter region, MCF-7 cell nuclear extract, and an excess of either nonlabeled competitor DNA containing the wild-type Sp consensus sequence or nonlabeled mutant oligonucleotide (Figure 5A). As indicated by the disappearance of the three band shifts, the wild-type oligonucleotide was able to successfully compete with the target DNA for the Sp transcription factors, whereas the mutant DNA was not. Furthermore, EMSA with an antibody specific for Sp1 resulted in the loss of the first band from the top of the gel, which was therefore identified as a consequence of the formation of a complex between c-*src* DNA and Sp1. Analysis using an Sp3-specific antibody resulted in the supershift of the second and third bands, showing their association with Sp3 binding. Normal rabbit IgG antibody did not affect the band shifts. Correspondingly, the unlabeled Oct1 oligonucleotide was able to compete with the labeled Oct1 probe for binding of the Oct1 transcription factor, as indicated by the disappearance of the protein−DNA band, while the Sp1 oligonucleotide did not (Figure 5B).

Sp1/3 Binding to c-src DNA in the Presence of MTM and MTM Analogues. To determine the ability of MTM and/or the MTM analogues to bind to and block the binding of Sp transcription factors to the c-*src* DNA, we performed EMSAs using the labeled 42 bp DNA fragment from the c-*src* promoter region, MCF-7 cell nuclear extract, and various concentrations of the desired compounds. The resulting EMSA autoradiographs are shown in Figure 5A. Treatment of the DNA target with 20 μM MTM (**1**) caused a significant decrease in all three Sp−DNA complex band shifts, while Sp binding was completely abolished at 100 μM. Conversely, Pre-B (**6**), 7-DM (**8**), and 4E-−K (**9**) were all unable to inhibit formation of the Sp−DNA complexes. Although SK (**7**) showed inhibition of Sp binding, it required a higher concentration than MTM. Experiments in which MTM and SK were used to treat a DNA probe for the GA2 site gave similar results (Figure 5B). Furthermore, at the concentrations tested, neither compound (MTM or SK) was able to inhibit binding of the Oct1 transcription factor, which is characterized by its preference for AT-rich DNA sequences (Figure 5C) (*40*). Surprisingly, use of 4C-K (**10**) caused no inhibition of Sp1/3 binding at 20 μM and only minimally inhibited formation of Sp−DNA complexes at 100 μM. This is interesting given its ability to bind to the 223 bp DNA target, thus producing footprints, several of which overlap with MTM footprints. Possible reasons for the reduced ability of SK and 4C-K to block Sp binding are discussed below.

Inhibition of c-src Promoter Activity by MTM and SK in Cancer Cells. To determine the ability of MTM and/or the MTM analogues to inhibit Sp-regulated transcription, the c-*src* promoter was cloned into a luciferase reporter vector (pGL3) and transfected into A549 cells. Incubation of the A549 cells with 100 nM MTM (**1**) or SK (**7**) resulted in a decrease of c-*src* promoter activity to about 30% of the control (Figure 6). This is similar to the reported decrease in c-*src* transcriptional activity obtained upon mutation of *both* the GC1 and GA2 sites (*38*), thus suggesting that both Sp binding sites are blocked by MTM and SK. All other analogues were inactive at the tested concentration (100 nM) (data not shown).

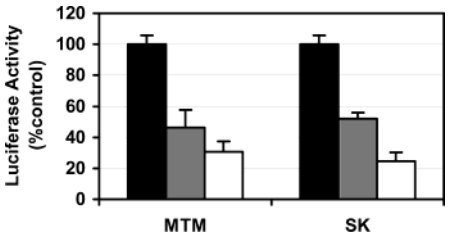

FIGURE 6: Effects of MTM and SK on c-*src* promoter activity. A549 cells were transfected with pGL3-SRC and pRL-CMV (control) vectors using cationic lipids (DOTAP). After 6 h, the transfection medium was removed, and cells were treated with MTM or SK. After 18 h, cells were lysed, and luciferase activity was determined using the dual luciferase assay system. Renilla luciferase activity was used to correct for variation in transfection efficiency. Each data point represents the mean ± SD of triplicate samples. Black bars = 0 nM, gray bars = 50 nM, and white bars = 100 nM. MTM = mithramycin (**1**) and SK = mithramycin SK (**7**).

Effects of MTM and MTM Analogues on Transcription of the c-src Gene in Cancer Cells. RT-PCR was used to determine the ability of MTM and/or the MTM analogues to decrease endogenous c-*src* expression. As shown in Figure 7, incubation of A549 cells with increasing concentrations (similar to those used in the luciferase and MTT assays) of MTM (**1**) or SK (**7**) led to a concomitant decrease in the production of c-*src* RNA (ca. 90% decrease at the highest concentration tested). Incubation with the other analogues had little effect on the levels of c-*src* RNA.

Antiproliferative Activity of the Selected Compounds against Human Cancer Cell Lines. To evaluate the biological activity, as well as to investigate their potential as anticancer drugs, MTM and the MTM analogues were used to treat various human cancer cell lines in MTT assays (Figure 8). A549 and H441 cells were tested against the complete set of analogues, and the results were similar to those seen in both the luciferase and RT-PCR experiments. That is, MTM (**1**) and SK (**7**) were active, while all other analogues were inactive. The remaining four cell lines, namely, H23, DU145, MDA-MB-23, and SW480, were treated only with MTM, SK, and 7-DM (**8**) (as a control for nonactivity). As above, MTM and SK were both able to decrease the number of viable cells in a dose-dependent manner to between 80% and 90%.

DISCUSSION

The nonreceptor protein tyrosine kinase (PTK) c-Src is one of the most prominent members of the Src family of related proteins. These ubiquitously expressed protein kinases are involved in signal transduction cascades controlling a variety of cellular processes, such as mitogenesis, proliferation, differentiation, motility, and adhesion (*42*, *43*). Src, which normally remains inactive, can be activated transiently during these normal cellular events or constitutively by abnormal events such as mutation (*43*, *44*). Besides its involvement in cancer progression, c-Src is known to be vital for the bone-resorbing function of osteoclasts, where it is

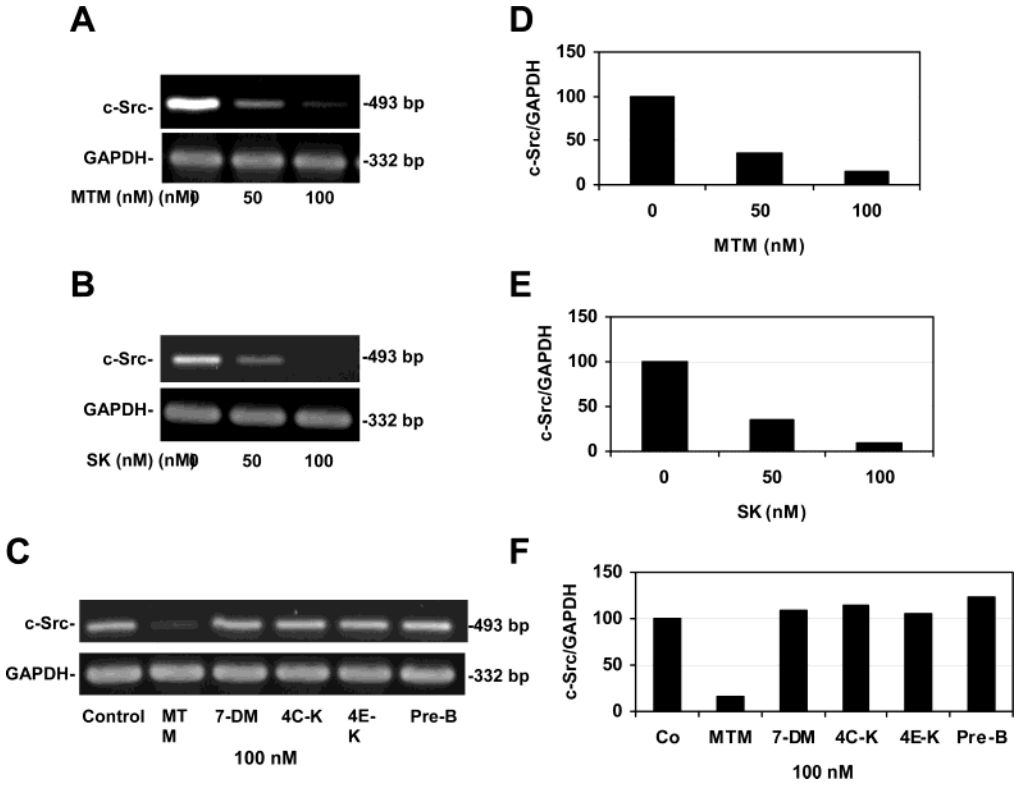

FIGURE 7: Effects of MTM and MTM analogues on c-*src* expression. A549 cells were treated with the indicated concentrations of MTM (panel A) and SK (panel B) or with the indicated compounds (100 nM) (panel C) for 24 h. Total RNA was isolated from control and drug-treated cells and analyzed by RT-PCR using c-*src*- and GAPDH-specific primers. Panels D, E, and F show densitometric analysis of the c-*src* RNA level corrected for the GAPDH RNA level for each treatment group. MTM = mithramycin (**1**), Pre-B = premithramycin B (**6**), SK = mithramycin SK (**7**), 7-DM = 7-demethylmithramycin (**8**), 4E-K = 4E-ketomithramycin (**9**), and 4C-K = 4C-ketodemycarosylmithramycin (**10**).

believed to be involved in the formation of ruffled borders (*45*, *46*). c-Src activity can be inhibited by different mechanisms: herbimycin A binds to the c-Src protein (*47*), while antisense RNA reduces the production of c-Src (*48*). Inhibition of c-*src* transcription can also be used to control c-Src activity. Therefore, compounds that inhibit c-*src* transcription are of considerable interest for both the treatment of cancer as well as of diseases in context with bone loss, such as hypercalcemia and osteoporosis.

It is known that transcription of c-*src* is Sp1 dependent (*22*). The results of our investigations demonstrate that mithramycin (MTM) inhibits the expression of the PTK c-Src by competing for the Sp1 binding site of the c-*src* promoter region. This provides additional insight into MTM's mode of action as an anticancer drug and illustrates for the first time one potential mechanism through which MTM affects the activity of osteoclasts. Furthermore, an effect of aureolic acid-type drugs on mitosis was recently postulated (*49*). As it has been demonstrated that c-Src is involved in mitosis (*43*), our results also provide further indirect evidence that MTM is affecting both nucleic acid synthesis as well as cell mitosis.

Given the ability of MTM to block the binding of Sp transcription factors to the c-*src* promoter, this gene was chosen as the target for the second goal of this work, which was to further characterize the SAR of MTM using several previously prepared MTM analogues. MTM is known to bind to the minor groove of GC-rich DNA as a Mg^{2+}−dimer complex (MTM:Mg^{2+} = 2:1) in which Mg^{2+} coordinates with the 1-O carbonyl oxygen and 9-O phenolate anion of each aglycon in the dimer (*6*). Sequence specificity is acquired by hydrogen bonding between the 8-O hydroxyl group and the guanine NH_2. Further DNA binding properties of the aureolic acid antibiotics have been intensively investigated by NMR and X-ray crystallographic studies (*6*, *7*, *50*−*52*), particularly in view of the role played by the oligosaccharide moieties. While these and other studies reveal that (1) the deoxysaccharide moieties of MTM extend across the entire minor groove with the A and B sugars crossing the phosphate backbone and lying near the major groove (*53*), (2) the C-D units of the trisaccharide chains of MTM, OLI, and CHR stack on the aromatic core of the dimer-partner aglycon, and (3) the intact C-D-E trisaccharide moiety is essential for dimer formation as well as optimal DNA binding, the roles of the C-7 alkyl side chain and of the C-3 polyoxygenated pentyl side chain are less well characterized. Thus, derivatives, which differ with respect to the sugar units of the trisaccharide chain or the alkyl side chains at C-7 and C-3, can be used to provide further insight into the SAR of the aureolic acid-type antitumor drugs.

Pre-B (**6**), the tetracyclic biosynthetic intermediate of the MTM pathway, which lacks the C-3 side chain, shows no noticeable DNA binding, does not block c-*src* expression, and is inactive in the cytotoxicity assays. Thus, this side chain is particularly important and seems to play a major role in DNA binding and biological activity of MTM. The importance of the 3-side chain can also be deduced from the observed results of the derivative with the shorter and slightly altered side chain, mithramycin SK (**7**). The indistinguishable footprint patterns observed for MTM and SK implied a

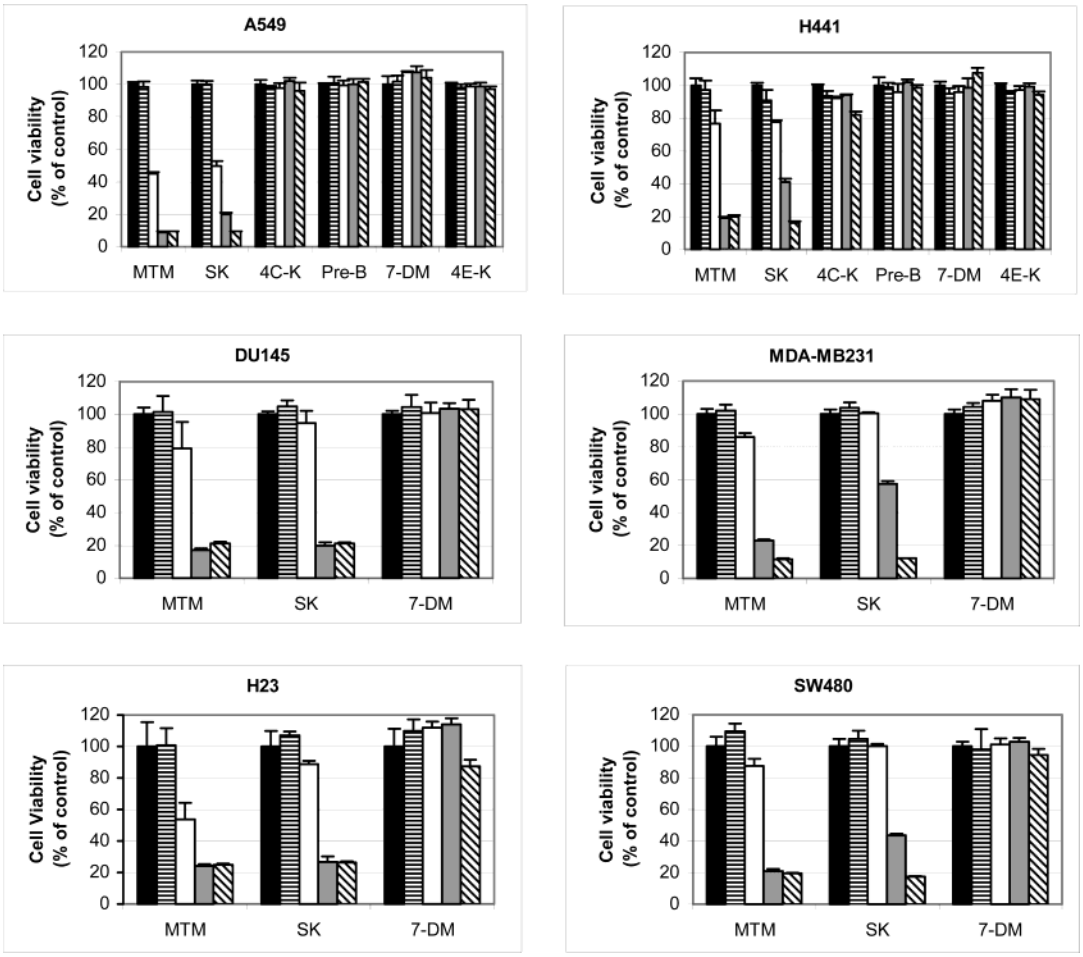

FIGURE 8: Antiproliferative activity of MTM analogues in human cancer cell lines. Cells were incubated with increasing concentrations of the indicated compounds. After 96 h, 25 μL of MTT (5 mg/mL in PBS) was added to each well, and the cells were incubated for 4 h. This was followed by overnight lysis at 37 °C. Absorbance was recorded at 570 nm on a microplate reader. Each treatment group was performed in triplicate. MTM = mithramycin (**1**), Pre-B = premithramycin B (**6**), SK = mithramycin SK (**7**), 7-DM = 7-demethylmithramycin (**8**), 4E-K = 4E-ketomithramycin (**9**), and 4C-K = 4C-ketodemycarosylmithramycin (**10**). Black bars = 0 nM, striped bars = 1 nM, white bars = 10 nM, gray bars = 100 nM, and diagonal bars = 1000 nM.

similar DNA binding affinity and specificity for these two compounds. However, further analysis using EMSA indicated that there is indeed a difference in their ability to inhibit the binding of Sp transcription factors to DNA. It is possible that the change in the side chain causes SK to bind slightly weaker to the DNA than MTM does, making it possible for Sp proteins to compete and dissociate SK−DNA complexes more effectively than MTM−DNA complexes. Even with this lesser binding ability, the promoter reporter, gene expression analysis, and cytotoxicity assays indicate that SK has inhibitory effects on c-*src* expression and cell growth similar to those of MTM in the tested cell lines. A possible explanation for this seemingly contradictory result is provided by several studies, which suggest that normal cells are more capable of recovering from MTM treatment than cancer cells due to their ability to take advantage of the period of dissociation of MTM from the DNA, while rapidly reproducing cells, such as cancer cells, cannot (*4*). Since SK binds to DNA with an identical specificity, but apparently not as tightly as MTM, this compound may possess a more optimized DNA binding/dissociation relationship and thus may be less toxic than MTM while maintaining similar concentrations of efficacy. Interestingly, the National Cancer Institute's sulforhodamine B-based anticancer screening of a panel of 60 different human tumor cell lines (*54*−*58*) revealed that in several cases this novel drug possessed a growth inhibitory effect (GI_{50}) of up to an order of magnitude better than MTM[2] (*31*). At the same time, toxicity assays show that SK exhibits an astounding 1500-fold decrease in in vitro toxicity (*31*). Although the current SAR study was unable to ascertain the mechanism through which SK exhibits enhanced activity, the results presented here do indicate that the modification of the 3-side chain as obtained for SK seems to be advantageous in terms of toxicity, and further refinement of this side chain may be profitable.

The importance of the substitution at the 7-position of the aureolic acid family of antitumor antibiotics is illustrated by the newer natural products UCH9 (**4**) and DUR (**5**), which possess a *sec*-butyl group in this position. This larger hydrophobic side chain (compared to a hydrogen in OLI and a methyl group in MTM and CHR) forces the sugars away from the DNA and replaces the D-sugar of UCH9 (corresponds to the E-sugar moiety of MTM, CHR, OLI, and DUR) in the minor groove (*59*). This replacement decreases the alteration of the surrounding DNA structure (the side chain

[2] E. Sausville, A. B. Mauger, and V. L. Narayanan, National Cancer Institute, Bethesda, MD, personal communication, 2000.

is less bulky than the E-sugar of CHR, MTM, etc.) and may be the reason for the lower observed anticancer activity of UCH9 compared to CHR and MTM (*60*). Besides the substitution at the 7-position, OLI also differs from CHR in that an isobutyryl is found in place of an acetyl group in the E-sugar. Nevertheless, these differences do not alter the DNA binding specificity of OLI compared to CHR since both compounds produce almost identical footprinting patterns (*5*). 7-Demethylmithramycin (**8**) is to MTM as OLI is to CHR (with respect to the aglycon) in that it also lacks the methyl group at the 7-position (see Figures 1 and 2). Surprisingly, however, in the case of 7-DM, we found that the removal of this methyl group led to the complete loss of binding to the c-*src* probe (Figure 4). The sugar side chains of OLI and CHR contain larger functional groups (acetyl, *O*-methyl groups) than are found in MTM. The increased interaction of these acetoxy and methoxy groups of the CHR/OLI sugars with DNA inhibits the rotational freedom of the saccharide functions and locks them into a specific formation (*61*), thus making the absence or presence of the 7-methyl group less crucial for their orientation. The saccharide chains in MTM do not contain such elements of rigidity and are therefore more flexible (*7*, *62*). This flexibility gives MTM the ability to bind more molecules to various oligonucleotides (*7*, *63*) than CHR by decreasing the space necessary for binding each dimeric complex. Our results here suggest that this flexibility of the trisaccharide chain of MTM renders the drug more dependent on the presence of the 7-methyl group for sterical positioning of the sugar chains for binding either to one another within the dimer complex or to the DNA itself. It follows that the lack of this important 7-methyl group in 7-DM makes DNA binding impossible (or drastically reduces DNA binding ability). As a consequence, no inhibition of Sp1−DNA formation was observed with 7-DM (EMSA, Figure 5).

As discussed above, MTM sugars are more flexible and possess greater freedom of movement than the bulkier sugars of CHR; therefore, MTM alters DNA structure less and is not as sensitive to groove dimension compared to CHR (*64*, *65*). Additionally, MTM has a faster off-rate from DNA than does CHR, since it lacks the increased interaction found between the CHR sugars and DNA (*61*). To further investigate the influence of the trisaccharide chain of MTM on its DNA binding properties, analogues specifically altered with respect to these lower saccharide moieties, namely, 4E-K (**9**) and 4C-K (**10**), were included in our study. In 4E-K, the equatorial OH group normally found in the 4-position of the mycarose moiety has been replaced by a keto group, while in 4C-K this mycarose moiety is completely missing. In addition, 4C-K contains a hydrated keto group instead of a hydroxyl group in the 4-position of the first sugar of the lower saccharide chain (sugar C). Thus, these compounds provided an opportunity to inspect particularly the role that the E-sugar in the trisaccharide chain plays in both the sequence specificity and binding affinity of MTM to the c-*src* promoter region. Upon examination of the footprint experiment with 4E-K (**9**), we were surprised to find that this compound seems to be completely unable to bind to DNA. It appears that the functional change at the 4E-position, from a H-bond donor to a H-bond acceptor, abolishes the ability of the trisaccharide chain to participate in the formation of a conformationally advantageous dimer complex suitable for DNA binding. Alternatively, the 4E-keto function may cause repulsions, which either do not allow a tight interaction of the dimer complex with the DNA or even prevent the formation of the 4E-K$-Mg^{2+}$ (2:1) complex. As a result, 4E-K was unable to inhibit either the formation of Sp1/Sp3−DNA complexes or c-*src* transcription. Also, 4E-K did not inhibit cancer cell growth in the MTT assays.

Conversely, by examining the results of the footprint experiments (Figure 4) with 4C-K (**10**), one can see that the complete removal of mycarose does not cause this analogue to lose its ability to bind to the DNA target. Consistent with a report from Behr et al. that the removal of sugar residues from the chromomycin molecule had little effect on the specificity of CHR analogues to DNA (*66*), the 4C-K footprints still correspond to regions of high GC content. However, there is a difference between MTM and 4C-K in the size, intensity, and location of the footprints (Figures 3 and 4). Although the smaller size of the 4C-K molecule, due to the loss of a sugar moiety, may account for the larger footprints compared to MTM, it is most likely the presence of the hydrate in the first sugar that is causing the sequence recognition discrepancy. The hydrate, which is in equilibrium with a keto group (*30*), affects both the proton donor/acceptor characteristics and the bulkiness of sugar C. Still, given the footprinting pattern observed with 4C-K, it was expected that this compound would be able to block the binding of Sp transcription factors to the c-*src* probe used in the gel shift assay. Surprisingly, as illustrated by the presence of all three Sp/DNA complex band shifts (Figure 5), this was not the case. It has been reported for various aureolic acid antibiotics that the dissociation rate between DNA and drug increases with each loss of a sugar group and that the faster the dissociation rate, the lower the ability of the drugs to block polymerase reactions (*66*). Accordingly, 4C-K may have a very fast off-rate; it may bind for a time period long enough to block the DNase reaction, i.e., a fast reaction, which is highly susceptible to changes in DNA structure (*67*, *68*), but not long enough to inhibit the formation of a DNA/Sp−protein complex. Alternatively, as suggested for SK, 4C-K may only weakly interact with the DNA, thus allowing Sp proteins to compete with and dissociate 4C-K−DNA complexes. The slight decrease in the formation of Sp/DNA complexes at 100 μM 4C-K may imply that, at higher concentrations, 4C-K has the ability to compete for the desired DNA binding sites, but the results of the RT-PCR, promoter reporter, and growth inhibition assays show that 4C-K does not bind tightly enough (or long enough) to the DNA to exhibit a decrease in the functionality of the c-*src* promoter or in the viability of the tested cell lines. This is not to say that this compound does not warrant further examination. Given that 4C-K binds to DNA with a closely related specificity and apparently a lot less tightly than MTM, this compound may prove to be less toxic than MTM, despite the fact that higher concentrations are necessary for efficacy. The difference in the footprint regions suggests that it is also possible that this compound may be applicable to other disease systems, including other cancers.

In summary, the studies reported here identify one potential mechanism by which MTM inhibits osteoclast-mediated bone resorption and exerts its anticancer activity, namely, through blocking the Sp1-dependent expression of the protein tyrosine kinase c-Src. With respect to the SAR

of MTM, the assayed MTM analogues show that subtle changes in the chemical structure of this drug cause enormous consequences for its biological activity. Our studies confirm the importance of the trisaccharide chain of MTM, in particular its E-sugar moiety, whose 4E-OH group seems to be essential for the formation of the drug−Mg^{2+}−DNA (2:1:1) complex. This work also reveals for the first time the importance of the 7-methyl group for the activity of MTM, which is probably due to its steric influence on the positioning of the saccharide chains in the dimer complex of the drug. Finally, the investigations show initial evidence for the importance of the highly functionalized, conformationally flexible 3-side chain of MTM and its contribution to the DNA binding, which has the potential to be even further refined in the future. The SAR studies were made possible by using combinatorial biosynthesis, which allowed us, in a relatively short period of time, to generate a number of MTM analogues, which would have been difficult or impossible to generate using other methods, such as chemical derivatization or total synthesis.

ACKNOWLEDGMENT

We thank Profs. C. Mendez and J. A. Salas and their team for enormous input in the generation of the here studied MTM analogues. Dr. Keith Bonham of the Saskatchewan Cancer Agency is kindly acknowledged for the gift of p0.54Src-CAT. Special thanks to Angie Collier for technical assistance.

REFERENCES

1. Jayasuriya, H., Lingham, R. B., Graham, P., Quamina, D., Herranz, L., Genilloud, O., Gagliardi, M., Danzeisen, R., Tomassini, J. E., Zink, D. L., Guan, Z. Q., and Singh, S. B. (2002) Durhamycim A, a potent inhibitor of HIV Tat transactivation, *J. Nat. Prod. 65*, 1091−1095.
2. Krishna, N. R., Miller, D. M., and Sakai, T. T. (1990) NMR and fluorometric characterization of mithramycin in aqueous solution, *J. Antibiot. 43*, 1543−1552.
3. Gause, G. F. (1975) Olivomycin, chromomycin, and mithramycin, in *Antibiotics III. Mechanism of action of antimicrobial antitumor agents* (Corcoran, J. W., and Hahn, F. E., Eds.) pp 197−202, Springer-Verlag, Berlin and New York.
4. Skarbek, J. D., and Speedie, M. K. (1981) Antitumor antibiotics of the aureolic acid group: Chromomycin A_3, mithramycin A, and olivomycin A, in *Antitumor compounds of natural origin: Chemistry and biochemistry* (Aszalos, A., Ed.) pp 191−235, CRC Press, Boca Raton, FL.
5. Fox, K. R., and Howarth, N. R. (1985) Investigations into the sequence-selective binding of mithramycin and related ligands to DNA, *Nucleic Acids Res. 13*, 8695−8714.
6. Sastry, M., and Patel, D. J. (1993) Solution structure of the mithramycin dimer-DNA complex, *Biochemistry 32*, 6588−6604.
7. Sastry, M., Fiala, R., and Patel, D. J. (1995) Solution structure of mithramycin dimers bound to partially overlapping sites on DNA, *J. Mol. Biol. 251*, 674−689.
8. Majee, S., Dasgupta, D., and Chakrabarti, A. (1999) Interaction of the DNA-binding antitumor antibiotics chromomycin and mithramycin with erythroid spectrin, *Eur. J. Biochem. 260*, 619−626.
9. Elias, E. G., and Evans, J. T. (1972) Mithramycin in the treatment of Paget's disease of bone, *J. Bone Joint Surg. 54-A*, 1730−1736.
10. Brown, J. H., and Kennedy, B. J. (1965) Mithramycin in the treatment of disseminated testicular neoplasms, *N. Engl. J. Med. 272*, 111−118.
11. Ryan, W. G., Schwartz, T. B., and Northrop, G. (1970) Experiences in the treatment of Paget's disease of bone with mithramycin, *J. Am. Med. Assoc. 213*, 1153−1157.
12. Robins, P. R., and Jowsey, J. (1973) Effect of mithramycin on normal and abnormal bone turnover, *J. Lab. Clin. Med. 82*, 576−586.
13. Dewick, P. M. (1997) *Medicinal natural products: A biosynthetic approach*, p 85, Wiley, Chichester, NY.
14. Aich, P., and Dasgupta, D. (1995) Role of magnesium ion in mithramycin-DNA interaction: Binding of mithramycin-Mg^{2+} complexes with DNA, *Biochemistry 34*, 1376−1385.
15. Majee, S., and Chakrabarti, A. (1999) Membrane interaction of an antitumor antibiotic, mithramycin, with anionic phospholipid vesicles, *Biochem. Pharmacol. 57*, 981−987.
16. Suske, G. (1999) The Sp-family of transcription factors, *Gene 238*, 291−300.
17. Chatterjee, S., Zaman, K., Ryu, H., Conforto, A., and Ratan, R. R. (2001) Sequence-selective DNA binding drugs mithramycin A and chromomycin A_3 are potent inhibitors of neuronal apoptosis induced by oxidative stress and DNA damage in cortical neurons, *Ann. Neurol. 49*, 345−354.
18. Nehls, M. C., Brenner, D. A., Gruss, H. J., Dierbach, H., Mertelsmann, R., and Herrmann, F. (1993) Mithramycin selectively inhibits collagen-alpha 1(I) gene expression in human fibroblast, *J. Clin. Invest. 92*, 2916−2921.
19. Blume, S. W., Snyder, R. C., Ray, R., Thomas, S., Koller, C. A., and Miller, D. M. (1991) Mithramycin inhibits Sp1 binding and selectively inhibits transcriptional activity of the dihydrofolate reductase gene in vitro and in vivo, *J. Clin. Invest. 88*, 1613−1621.
20. Snyder, R. C., Ray, R., Blume, S., and Miller, D. M. (1991) Mithramycin blocks transcriptional initiation of the c-myc P1 and P2 promoters, *Biochemistry 30*, 4290−4297.
21. Ray, R., Snyder, R. C., Thomas, S., Koller, C. A., and Miller, D. M. (1989) Mithramycin blocks protein binding and function of the SV40 early promoter, *J. Clin. Invest. 83*, 2003−2007.
22. Ritchie, S., Boyd, F. M., Wong, J., and Bonham, K. (2000) Transcription of the human c-Src promoter is dependent on Sp1, a novel pyrimidine binding factor SPy, and can be inhibited by triplex-forming oligonucleotides, *J. Biol. Chem. 275*, 847−854.
23. Irby, R. B., and Yeatman, T. J. (2000) Role of Src expression and activation in human cancer, *Oncogene 19*, 5636−5642.
24. Biscardi, J. S., Tice, D. A., and Parsons, S. J. (1999) c-Src, receptor tyrosine kinases, and human cancer, *Adv. Cancer Res. 76*, 61−119.
25. Soriano, P., Montgomery, C., Geske, R., and Bradley, A. (1991) Targeted disruption of the c-src proto-oncogene leads to osteopetrosis in mice, *Cell 64*, 693−702.
26. Hall, T. J., Schaeublin, M., and Chambers, T. J. (1993) The majority of osteoclasts require mRNA and protein synthesis for bone resorption in vitro, *Biochem. Biophys. Res. Commun. 195*, 1245−1253.
27. Calabresi, P., and Chabner, B. A. (1991) Antineoplastic agents, in *The pharmacological basis of therapeutics* (Goodman-Gilman, A., Ed.) pp 1209−1263, Pergamon Press, Oxford, U.K.
28. Gonzalez, A., Remsing, L. L., Lombo, F., Fernandez, M. J., Prado, L., Brana, A. F., Kunzel, E., Rohr, J., Mendez, C., and Salas, J. A. (2001) The mtmVUC genes of the mithramycin gene cluster in Streptomyces argillaceus are involved in the biosynthesis of the sugar moieties, *Mol. Gen. Genet. 264*, 827−835.
29. Lozano, M. J. F., Remsing, L. L., Quiros, L. M., Brana, A. F., Fernandez, E., Sanchez, C., Mendez, C., Rohr, J., and Salas, J. A. (2000) Characterization of two polyketide methyltransferases involved in the biosynthesis of the antitumor drug mithramycin by Streptomyces argillaceus, *J. Biol. Chem. 275*, 3065−3074.
30. Remsing, L. L., Garcia-Bernardo, J., Gonzalez, A., Kunzel, E., Rix, U., Brana, A. F., Bearden, D. W., Mendez, C., Salas, J. A., and Rohr, J. (2002) Ketopremithramycins and ketomithramycins, four new aureolic acid-type compounds obtained upon inactivation of two genes involved in the biosynthesis of the deoxysugar moieties of the antitumor drug mithramycin by Streptomyces argillaceus, reveal novel insights into post-PKS tailoring steps of the mithramycin biosynthetic pathway, *J. Am. Chem. Soc. 124*, 1606−1614.
31. Remsing, L. L., Gonzalez, A. M., Nur-e-Alam, M., Fernandez-Lonzano, M. J., Brana, A. F., Rix, U., Oliveira, M. A., Mendez, C., Salas, J. A., and Rohr, J. (2003) Mithramycin SK, a novel antitumor drug with improved therapeutic index, mithramycin SA, and demycarosyl-mithramycin SK: Three new products generated in the mithramycin producer Streptomyces argillaceus through combinatorial biosynthesis, *J. Am. Chem. Soc. 125*, 5745−5753.
32. Prado, L., Fernandez, E., Weissbach, U., Blanco, G., Quiros, L. M., Brana, A. F., Mendez, C., Rohr, J., and Salas, J. A. (1999)

Oxidative cleavage of premithramycin B is one of the last steps in the biosynthesis of the antitumor drug mithramycin, *Chem. Biol. 6*, 19−30.
33. Carpenter, M. L., Marks, J. N., and Fox, K. R. (1993) DNA-sequence binding preference of the GC-selective ligand mithramycin. Deoxyribonuclease-I/deoxyribonuclease-II and hydroxy-radical footprinting at CCCG, CCGC, CGGC, GCCC and GGGG flanked by (AT)n and An.Tn, *Eur. J. Biochem. 215*, 561−566.
34. Chen, G., Wang, G. Y., Li, X., Waters, B., and Davies, J. (2000) Enhanced production of microbial metabolites in the presence of dimethyl sulfoxide, *J. Antibiot. 53*, 1145−1153.
35. Cons, B. M., and Fox, K. R. (1990) The GC-selective ligand mithramycin alters the structure of (AT)n sequences flanking its binding sites, *FEBS Lett. 264*, 100−104.
36. Cons, B. M., and Fox, K. R. (1990) Footprinting studies of sequence recognition by mithramycin, *Anti-Cancer Drug Des. 5*, 93−97.
37. Cons, B. M., and Fox, K. R. (1991) Effects of the antitumor antibiotic mithramycin on the structure of repetitive DNA regions adjacent to its GC-rich binding site, *Biochemistry 30*, 6314−6321.
38. Bonham, K., and Fujita, D. J. (1993) Organization and analysis of the promoter region and 5′ noncoding exons of the human c-src proto-oncogene, *Oncogene 8*, 1973−1981.
39. McGuffie, E. M., and Catapano, C. V. (2002) Design of a novel triple helix-forming oligodeoxyribonucleotide directed to the major promoter of the c-myc gene, *Nucleic Acids Res. 30*, 2701−2709.
40. Kilwinski, J., Baack, M., Heiland, S., and Knippers, R. (1995) Transcription factor Oct1 binds to the AT-rich segment of the Simian virus 40 replication origin, *J. Virol. 69*, 575−578.
41. Catapano, C. V., McGuffie, E. M., Pacheco, D., and Carbone, G. M. (2000) Inhibition of gene expression and cell proliferation by triple helix-forming oligonucleotides directed to the c-myc gene, *Biochemistry 39*, 5126−5138.
42. Furstoss, O., Dorey, K., Simon, V., Barila, D., Superti-Furga, G., and Roche, S. (2002) c-Abl is an effector of Src for growth factor-induced c-myc expression and DNA synthesis, *EMBO J. 21*, 514−524.
43. Bjorge, J. D., Jakymiw, A., and Fujita, D. J. (2000) Selected glimpses into the activation and function of Src kinase, *Oncogene 19*, 5620−5635.
44. Irby, R. B., Mao, W., Coppola, D., Kang, J., Loubeau, J. M., Trudeau, W., Karl, R., Fujita, D. J., Jove, R., and Yeatman, T. J. (1999) Activating SRC mutation in a subset of advanced human colon cancers, *Nat. Genet. 21*, 187−190.
45. Hall, T. J., Schaeublin, M., and Missbach, M. (1994) Evidence that c-src is involved in the process of osteoclastic bone resorption, *Biochem. Biophys. Res. Commun. 199*, 1237−1244.
46. Mundy, G. R. (1993) Cytokines and growth factors in the regulation of bone remodeling, *J. Bone Miner. Res. 8*, S505−S510.
47. Yoneda, T., Lowe, C., Lee, C. H., Gutierrez, G., Niewolna, M., Williams, P. J., Izbicka, E., Uehara, Y., and Mundy, G. R. (1993) Herbimycin A, a pp60c-Src tyrosine kinase inhibitor, inhibits osteoclastic bone resorption in vitro and hypercalcemia in vivo, *J. Clin. Invest. 91*, 2791−2795.
48. Karni, R., Jove, R., and Levitzki, A. (1999) Inhibition of pp60c-Src reduces Bcl-XL expression and reverses the transformed phenotype of cells overexpressing EGF and HER-2 receptors, *Oncogene 18*, 4654−4662.
49. Rabow, A. A., Shoemaker, R. H., Sausville, E. A., and Covell, D. G. (2002) Mining the National Cancer Institute's tumor-screening database: Identification of compounds with similar cellular activities, *J. Med. Chem. 45*, 818−840.
50. Silva, D. J., and Kahne, D. E. (1993) Studies of the 2:1 chromomycin A_3−Mg^{2+} complex in methanol: Role of the carbohydrates in complex formation, *J. Am. Chem. Soc. 115*, 7962−7970.
51. Silva, D. J., Goodnow, R., Jr., and Kahne, D. (1993) The sugars in chromomycin A_3 stabilize the Mg(2+)-dimer complex, *Biochemistry 32*, 463−471.
52. Gao, X. L., Mirau, P., and Patel, D. J. (1992) Structure refinement of the chromomycin dimer-DNA oligomer complex in solution, *J. Mol. Biol. 223*, 259−279.
53. Huang, H. W., Li, D., and Cowan, J. A. (1995) Biostructural chemistry of magnesium. Regulation of mithramycin-DNA interactions by Mg^{2+} coordination, *Biochimie 77*, 729−738.
54. Boyd, M. R. (1989) Status of the NCI preclinical antitumor drug discovery screen, *Princ. Pract. Oncol. 3*, 1−12.
55. Boyd, M. R. (1995) Some practical considerations and applications of the National Cancer Institute in vitro anticancer drug discovery screen, *Drug Dev. Res. 34*, 91−109.
56. Boyd, M. R. (1997) The NCI in vitro anticancer drug discovery screen. Concept, implementation, and operation, 1985−1995, in *Anticancer drug development guide: Preclinical screening, clinical trials, and approval* (Teicher, B., Ed.) pp 23−42, Humana Press, Totowa, NJ.
57. Monks, A., Scudiero, D., Skehan, P., Shoemaker, R., Paull, K., Vistica, D., Hose, C., Langley, J., Cronise, P., and Vaigro-Wolff, A. (1991) Feasibility of a high-flux anticancer drug screen using a diverse panel of cultured human tumor cell lines, *J. Natl. Cancer Inst. 83*, 757−766.
58. Skehan, P., Storeng, R., Scudiero, D., Monks, A., McMahon, J., Vistica, D., Warren, J. T., Bokesch, H., Kenney, S., and Boyd, M. R. (1990) New colorimetric cytotoxicity assay for anticancer-drug screening, *J. Natl. Cancer Inst. 82*, 1107−1112.
59. Katahira, R., Katahira, M., Yamashita, Y., Ogawa, H., Kyogoku, Y., and Yoshida, M. (1998) Solution structure of the novel antitumor drug UCH9 complexed with $d(TTGGCCAA)_2$ as determined by NMR, *Nucleic Acids Res. 26*, 744−755.
60. Ogawa, H., Yamashita, Y., Katahira, R., Chiba, S., Iwasaki, T., Ashizawa, T., and Nakano, H. (1998) UCH9, a new antitumor antibiotic produced by Streptomyces: I. Producing organism, fermentation, isolation and biological activities, *J. Antibiot. 51*, 261−266.
61. Banville, D. L., Keniry, M. A., and Shafer, R. H. (1990) NMR investigation of mithramycin A binding to $d(ATGCAT)_2$: a comparative study with chromomycin A_3, *Biochemistry 29*, 9294−9304.
62. Keniry, M. A., Owen, E. A., and Shafer, R. H. (2000) The three-dimensional structure of the 4:1 mithramycin:d(ACCCGGGT)-(2) complex: evidence for an interaction between the E saccharides, *Biopolymers 54*, 104−114.
63. Keniry, M. A., Banville, D. L., Simmonds, P. M., and Shafer, R. H. (1993) Nuclear magnetic resonance comparison of the binding sites of mithramycin and chromomycin on the self-complementary oligonucleotide $d(ACCCGGGT)_2$. Evidence that the saccharide chains have a role in sequence specificity, *J. Mol. Biol. 231*, 753−767.
64. Chakrabarti, S., Bhattacharyya, D., and Dasgupta, D. (2002) Interaction of mithramycin and chromomycin A_3 with $d(TAGC-TAGCTA)_2$: Role of sugars in antibiotic-DNA recognition, *J. Phys. Chem. 106*, 6947−6953.
65. Chakrabarti, S., Bhattacharyya, D., and Dasgupta, D. (2001) Structural basis of DNA recognition by anticancer antibiotics, chromomycin A(3), and mithramycin: Roles of minor groove width and ligand flexibility, *Biopolymers 56*, 85−95.
66. Behr, W., Honikel, K., and Hartmann, G. (1969) Interaction of the RNA polymerase inhibitor chromomycin with DNA, *Eur. J. Biochem. 9*, 82−92.
67. Fox, K. R., and Waring, M. J. (1984) DNA structural variations produced by actinomycin and distamycin as revealed by DNAase I footprinting, *Nucleic Acids Res. 12*, 9271−9285.
68. Drew, H. R., and Travers, A. A. (1984) DNA structural variations in the E. coli tyrT promoter, *Cell 37*, 491−502.
69. Bonham, K., Ritchie, S. A., Dehm, S. M., Snyder, K., and Boyd, F. M. (2000) An alternative, human SRC promoter and its regulation by hepatic nuclear factor-1alpha, *J. Biol. Chem. 275*, 37604−37611.

BI034091Z